

◆◆ Introduction

If a polycrystalline film of a metal is placed in a vapour containing another metal, then atoms from the vapour diffuse into the film along the grain boundaries separating the crystals. The boundaries are observed to move and this motion is known as diffusion induced grain boundary motion. The newly created crystal that is produced behind the advancing grain is different from that in front as it has metal diffused from the vapour deposited in it see [7].

We consider the physical set up of a plate of metal immersed in a vapour see Figure 1 in which the dashed line represents the position of the grain boundary at some initial time $t = 0$, while the solid line denotes its position after some time $t > 0$. The region of new crystalline structure created behind the evolving boundary is depicted by the shaded area.

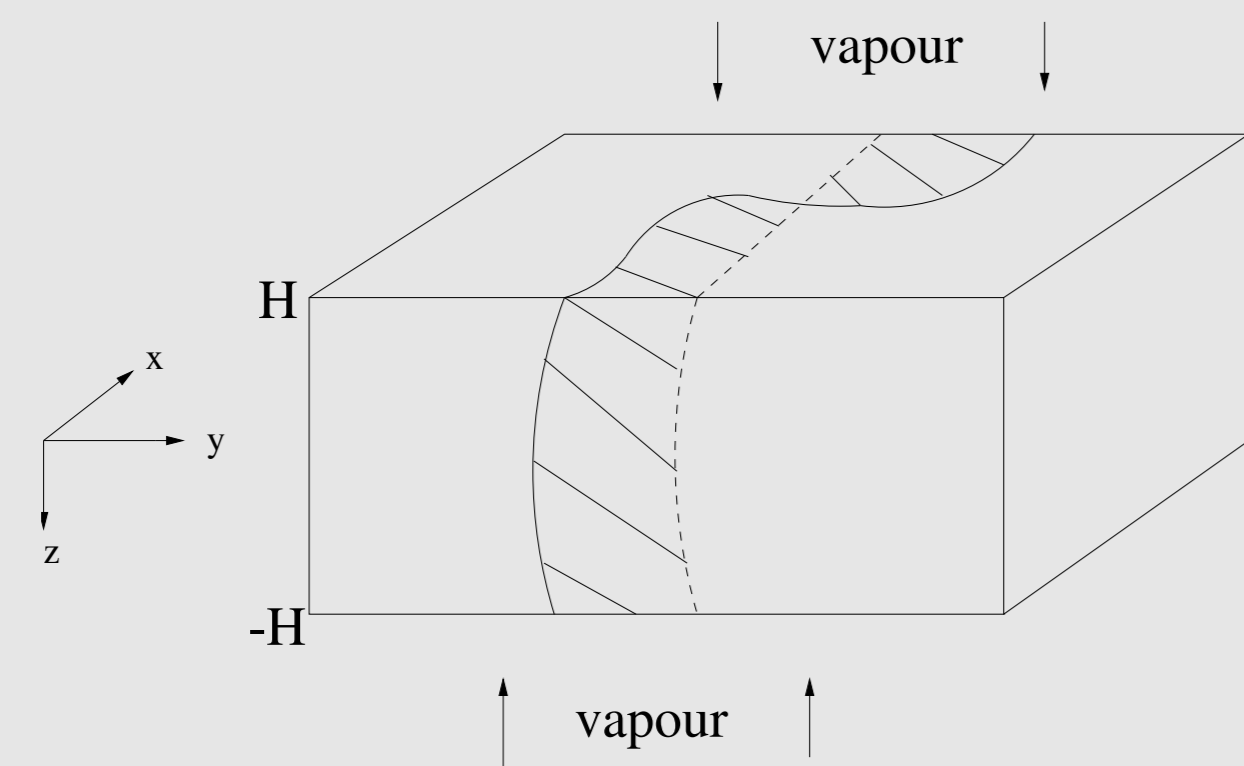
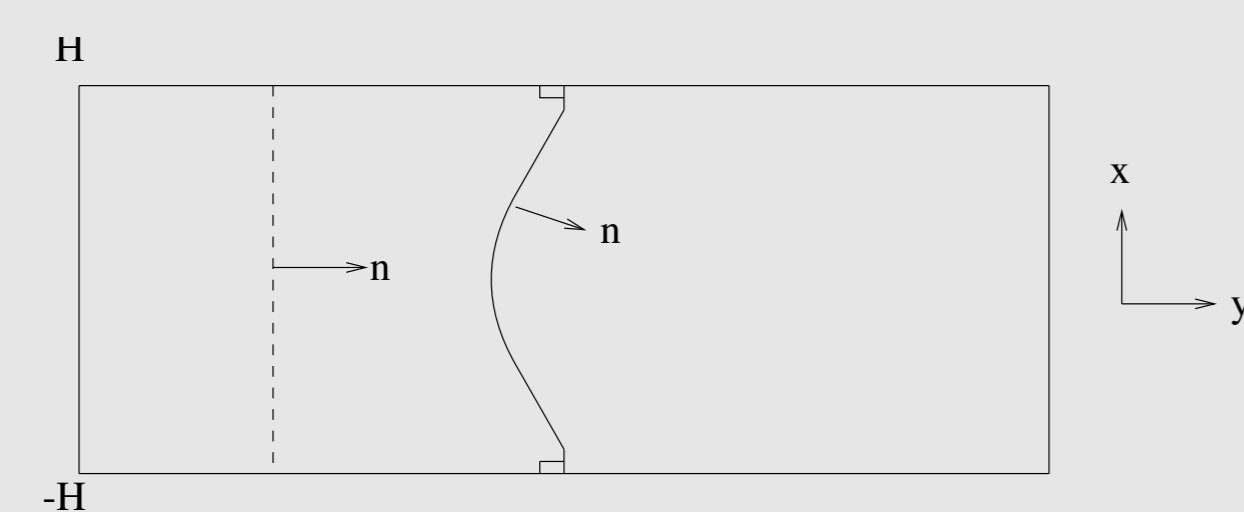


Figure 1: Physical set-up

We consider two dimensional reductions of this problem; one that is independent of the y direction and the other that is independent of the z direction.

◆◆ Uni-directional models

We assume independence of the y direction in Figure 1 and consider a grain boundary that spans the film. The boundary motion we consider is monotone in one direction.



◆ Phase field model

We consider the double obstacle phase field model presented in [1]

$$\rho\varphi_t - \Delta\varphi - \frac{1}{\varepsilon^2}\varphi + \beta(\varphi) + \frac{\pi f(u)}{4\varepsilon} \geq 0 \quad (1)$$

$$\varepsilon u_t = \frac{2}{\pi} \nabla \cdot ((1 - \varphi^2) \nabla u) \quad (2)$$

where ρ is a given positive, non-dimensional material constant and

$$\beta(r) = \begin{cases} (-\infty, 0] & \text{if } r = -1 \\ 0 & \text{if } |r| < 1 \\ [0, \infty) & \text{if } r = 1. \end{cases}$$

In the above model the grain boundary is modelled as a diffuse interface with width $\mathcal{O}(\varepsilon)$ for $\varepsilon \ll 1$. In this diffuse interface $|\varphi| < 1$ while on either side it takes either the value 1 or -1 . The variable u , lying in the range $0 \leq u \leq 1$, represents the concentration of solute atoms in the film.

We impose the boundary conditions

$$\frac{\partial\varphi}{\partial\mathbf{n}} = 0, \quad (1 - \varphi^2) \frac{\partial u}{\partial\mathbf{n}} = \alpha(1 - \varphi^2)(1 - u) \quad (3)$$

where α is a large positive number. The flux boundary condition for the concentration implies that the vapour can only enter the film through the grain boundary.

- The existence of a weak solution (that is unique in one dimension) to the phase field system (1)-(3) was proved in [2].
- A finite element discretization of (1)-(3) is studied in [3] where the approximate solutions are shown to convergence to a weak solution of the model.

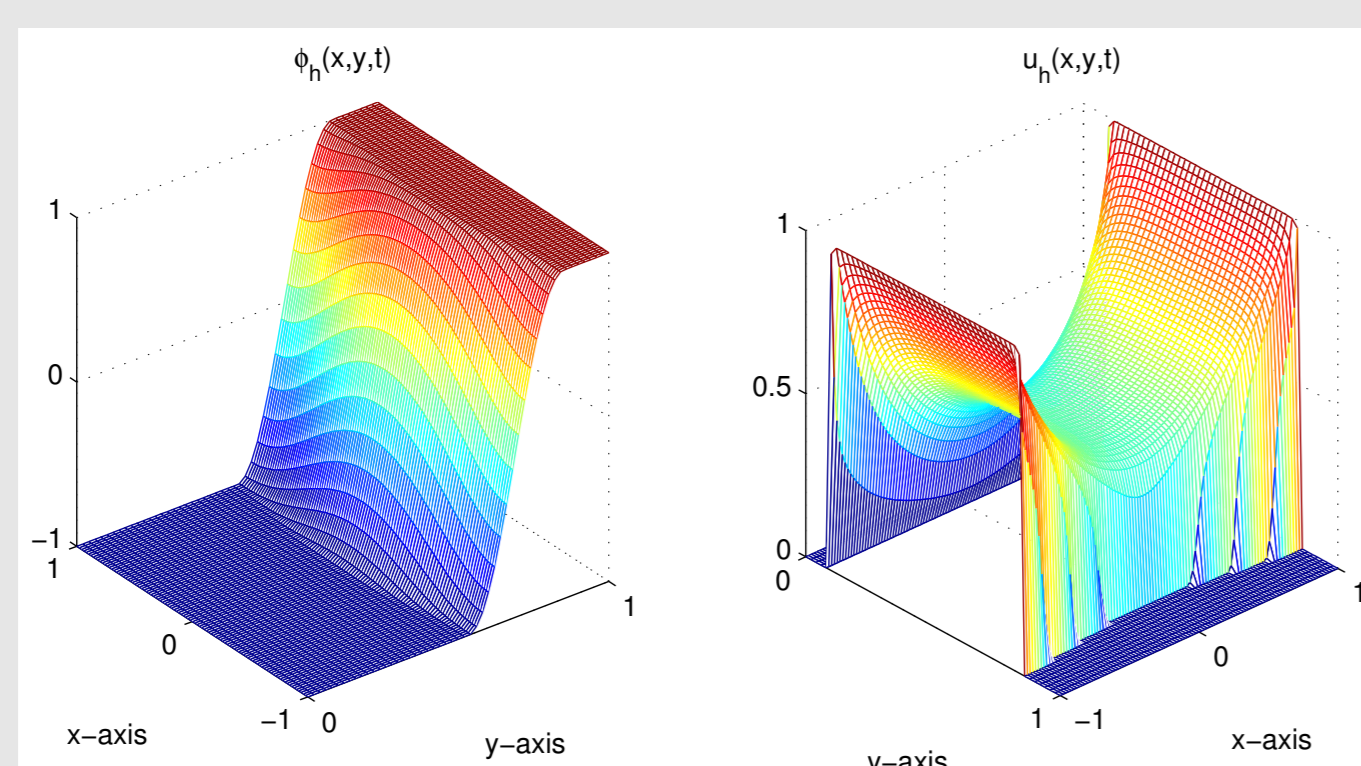


Figure 3: The phase field solutions φ_h and u_h at time $t = 0.25$.

◆ Sharp interface model

In [5] formal asymptotics on the phase field model for $\varepsilon \rightarrow 0$ are used to obtain the following sharp interface model

$$\rho V = \kappa + f(u) \quad (4)$$

$$\varepsilon_i u_t = u_{ss} - V u (1 + \varepsilon_2 \kappa) \quad (5)$$

where V , κ and s are respectively the normal velocity, the curvature and the arc-length of the sharp interface and $\varepsilon_i = \mathcal{O}(\varepsilon)$ $i = 1, 2$.

- A local existence/uniqueness result for (4), (5) is presented in [8].
- Parametrising the interface yields the following model that is studied in [3]

$$\mathbf{X} : [0, 1] \times [0, T] \rightarrow \mathbb{R}^2, \quad (p, t) \rightarrow \mathbf{X}(p, t) = (x(p, t), y(p, t))$$

$$\rho \mathbf{X}_t = \frac{\mathbf{X}_{pp}}{|\mathbf{X}_p|^2} + f(u) \frac{\mathbf{X}_p^\perp}{|\mathbf{X}_p|} \quad (6)$$

$$\varepsilon_i u_t = \frac{1}{|\mathbf{X}_p|} \left(\frac{u_p}{|\mathbf{X}_p|} \right)_p - u V (1 + \varepsilon_2 (\rho V - f(u))) \quad (7)$$

where $\mathbf{V} = \frac{\mathbf{X}_t \cdot \mathbf{X}_p^\perp}{|\mathbf{X}_p|}$ and $(\alpha_1, \alpha_2)^\perp = (\alpha_2, -\alpha_1)$.

- In [3] the model (6), (7) is discretized using mass lumping to give a semi-implicit difference scheme yielding three tri-diagonal systems that can be solved directly.
- Simulations obtained by solving the sharp interface and phase field discretizations show good agreement between the two models, see Figures 4 and 5. In these figures the phase field solutions are contour plots of φ_h and plots of the function obtained by averaging u_h across the interface. While the sharp interface solutions show a '*' plotted at every 20th node of the discretization.

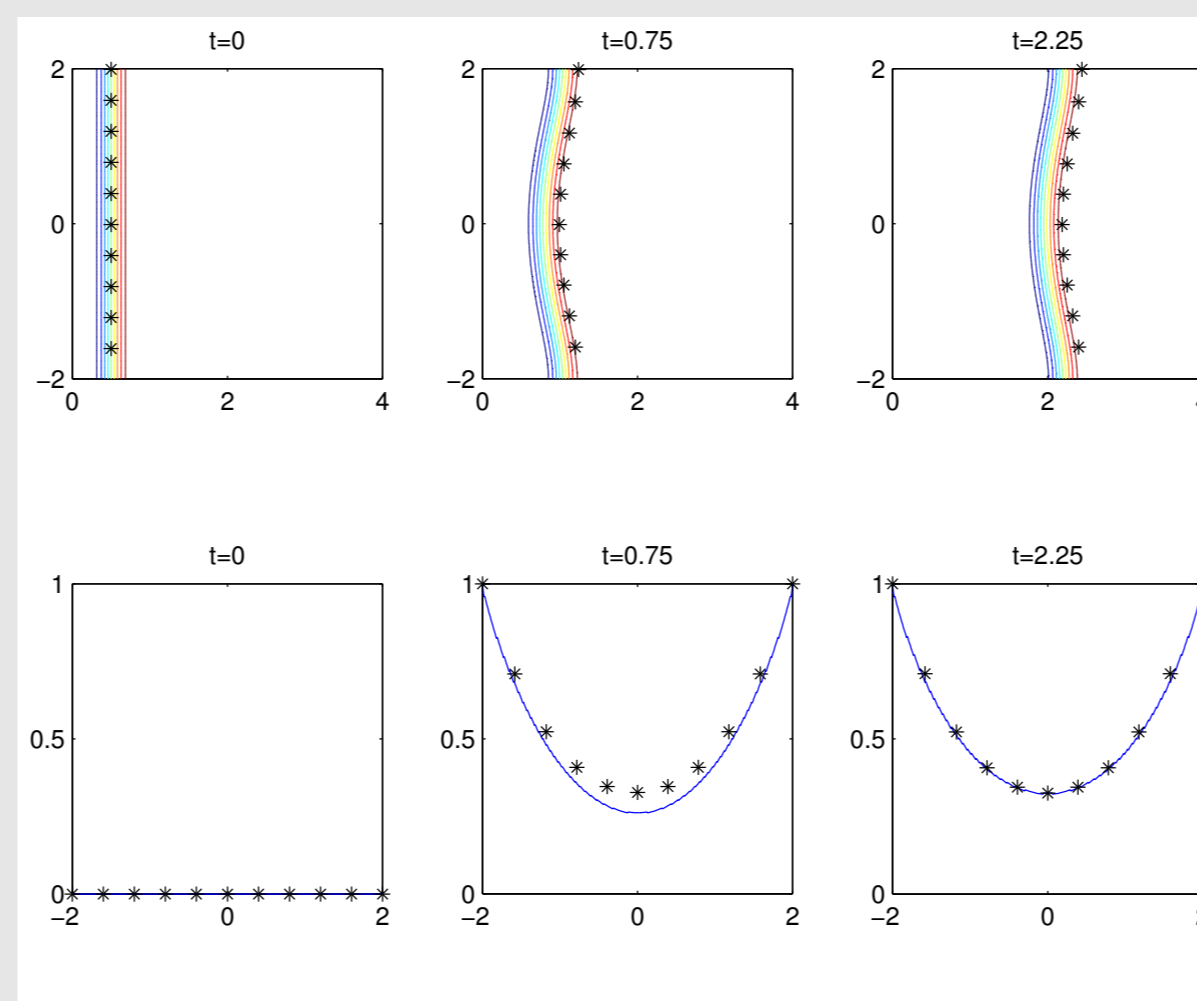


Figure 4: Comparisons of phase field and sharp interface evolutionary uni-directional solutions, $\rho = 0.4$, $H = 2$.

- The existence of travelling wave solutions of (4), (5) are obtained in [5].

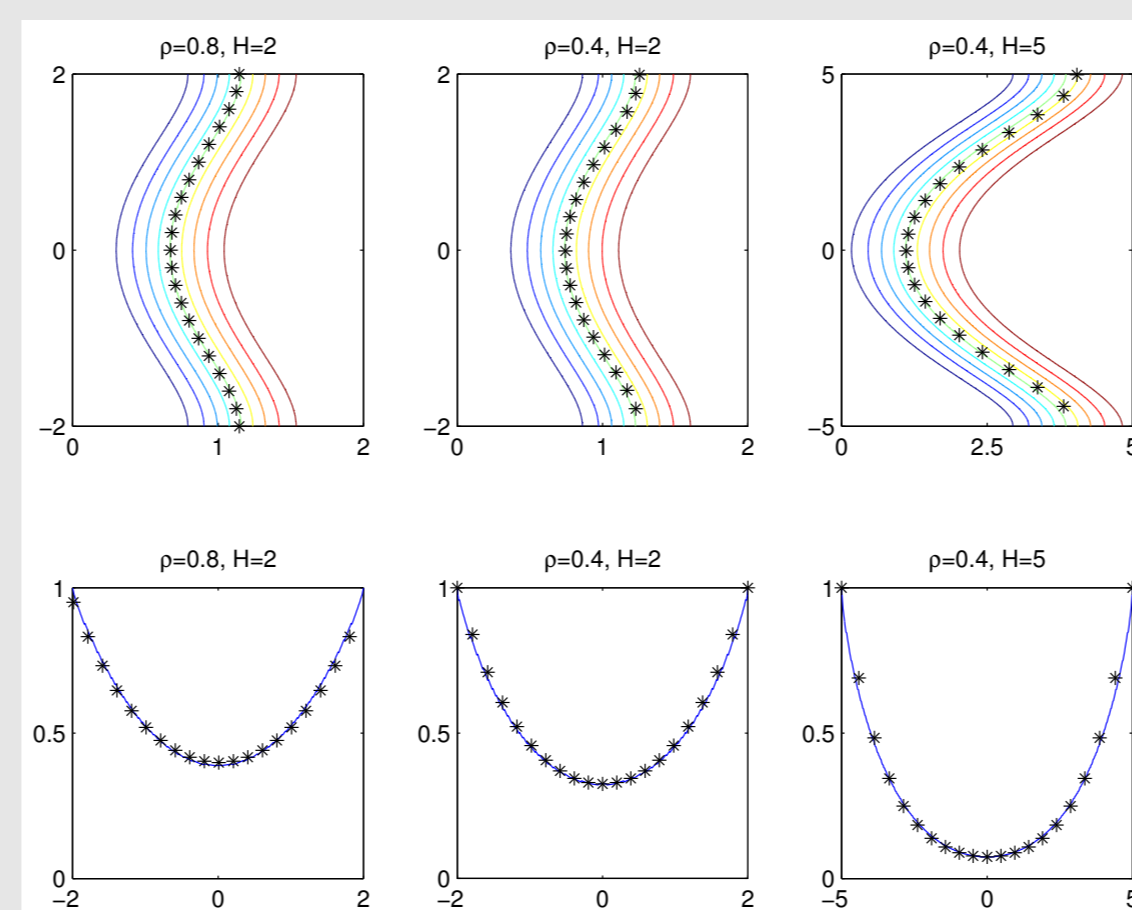


Figure 5: Comparisons of phase field and sharp interface travelling wave solutions.

◆◆ Bi-directional thin film models

For a thin film (H small in Figure 1) we assume independence of the z -direction and reduce the problem to a two-dimensional one for $\Omega \subset \mathbb{R}^2$ where Ω corresponds to the top face of the film. We consider grain boundaries that either span Ω or take the form of simple closed curves. We assume that diffusion takes place very rapidly so that $u(\mathbf{x}, t) = 1$ if the grain boundary has passed through the point $\mathbf{x} \in \Omega$.

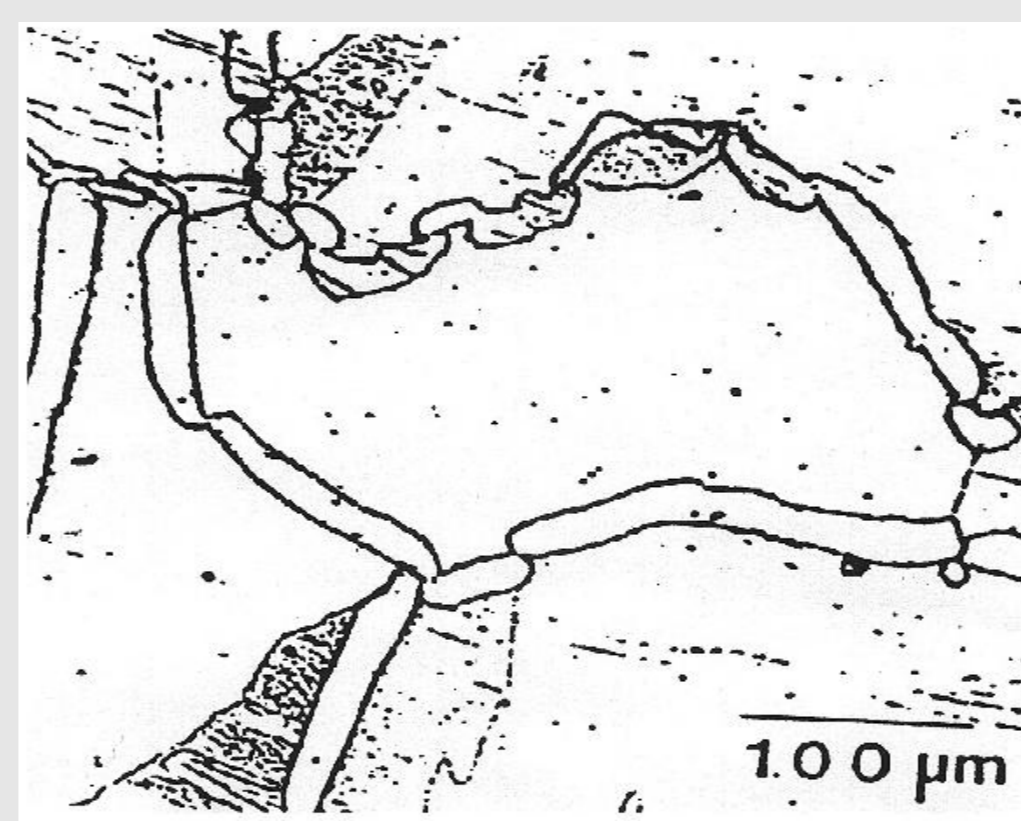


Figure 6: Diffusion induced grain boundary motion in foils of Fe that were exposed to Zn from a 90% Fe and 10% Zn source, see [7].

- Following the ideas introduced in [6] we propose the following model for bi-directional grain boundary motion in thin films

$$V = \kappa - [u]_\Gamma \quad (8)$$

$$u(\mathbf{x}, t) = \begin{cases} 1 & \forall (\mathbf{x}, t) \text{ such that } \mathbf{x} \in \Gamma(\bar{t}) \text{ for some } \bar{t} \leq t \\ 0 & \text{otherwise.} \end{cases} \quad (9)$$

- Here $[u]_\Gamma$ denotes the jump in concentration across the interface.
- In [4] sharp interface, phase field and level set models are proposed for bi-directional grain boundary motion in thin films. Numerical approximations and computational results are presented.

◆ Sharp interface model

A parameterised form of the sharp interface model (8), (9) is the following

$$\mathbf{X}_t = \frac{\mathbf{X}_{pp}}{|\mathbf{X}_p|^2} - [u]_\Gamma \frac{\mathbf{X}_p^\perp}{|\mathbf{X}_p|}$$

$$u(\mathbf{x}, t) = \begin{cases} 1 & \text{if } \exists \bar{t} \leq t : \mathbf{X}(\bar{t}) = \mathbf{x} \\ 0 & \text{otherwise.} \end{cases}$$

- To discretize this model we introduce a **background** uniform mesh. For any $\mathbf{x} \in \Omega$ we define $(\mathbf{x})^*$ to be its nearest node on the mesh.
- For $0 \leq \delta \ll 1$, we set $[u]_\Gamma = U_h^n((\mathbf{X}_j^n + \delta \mathbf{n})^*) - U_h^n((\mathbf{X}_j^n - \delta \mathbf{n})^*)$.
- At each time step we set $u_h^n((\mathbf{x})^*) = 1$ if the **background interface** $(\mathbf{X}_j^n)^*$ passes through the mesh point $(\mathbf{x})^*$.
- Figure 7 shows the evolution of a single closed curve grain boundary. The lefthand plot shows the grain boundary evolving in time to some final time $t = 12$. The righthand plot shows a contour plot of the concentration at this final time where $u = 1$ in the region between the two curves and $u = 0$ otherwise.

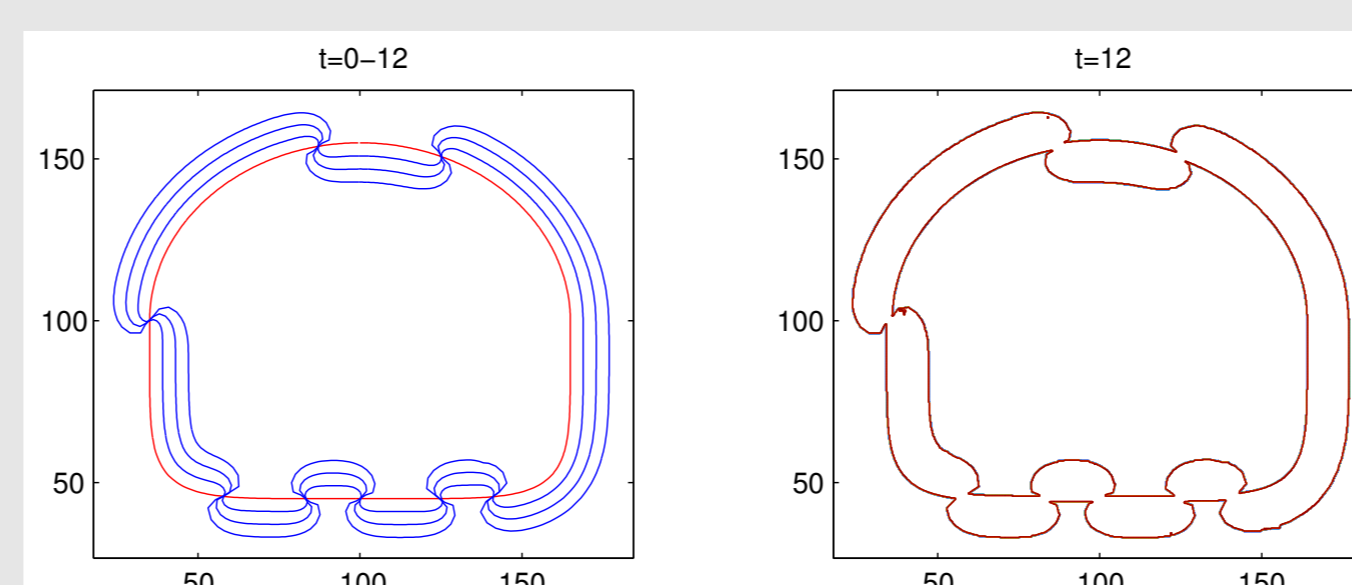


Figure 7: Evolutionary sharp interface simulation of a closed curve grain boundary.

◆ Phase field model

We propose a phase field model for thin film bi-directional grain boundary motion

$$\varphi_t - \Delta\varphi - \frac{1}{\varepsilon^2}\varphi + \beta(\varphi) - \frac{\pi \mathcal{F}[u, \varphi]}{4\varepsilon} \geq 0 \quad (10)$$

$$\gamma u_t + \tilde{\beta}(u) - (1 - \varphi^2) \geq 0 \quad (11)$$

where $\mathcal{F}[u, \varphi] = u(\mathbf{x} + \delta_\varphi^+ \mathbf{n}_\varphi) - u(\mathbf{x} - \delta_\varphi^- \mathbf{n}_\varphi)$ with

$$\mathbf{n}_\varphi = \frac{\nabla\varphi}{|\nabla\varphi|}, \quad \delta_\varphi^\pm = \min_{r \in \mathbb{R}^+} \{ |\varphi(\mathbf{x} \pm r \mathbf{n}_\varphi)| = \pm 1 \}$$

and

$$\tilde{\beta}(r) = \begin{cases} 0 & \text{if } r < 1 \\ [0, \infty) & \text{if } r = 1 \\ \infty & \text{if } r > 1. \end{cases}$$

- Equation (10) is a double obstacle Allen Cahn equation with a non local forcing term $\mathcal{F}[u, \varphi]$ that mimics the jump in concentration across the interfacial region and (11) is a time relaxation of (9) with relaxation time $\gamma \ll 1$.
- We discretize (10), (11) using a standard finite element discretization.

- Figure 8 shows an initially straight grain boundary that spans Ω evolving toward a stationary arc solution described in [6]. The lefthand subplot displays contour plots of the phase field solution φ_h at times $t = 0, 2.5, 7.5$ and 4 while the righthand plot displays the concentration u_h at the final time.

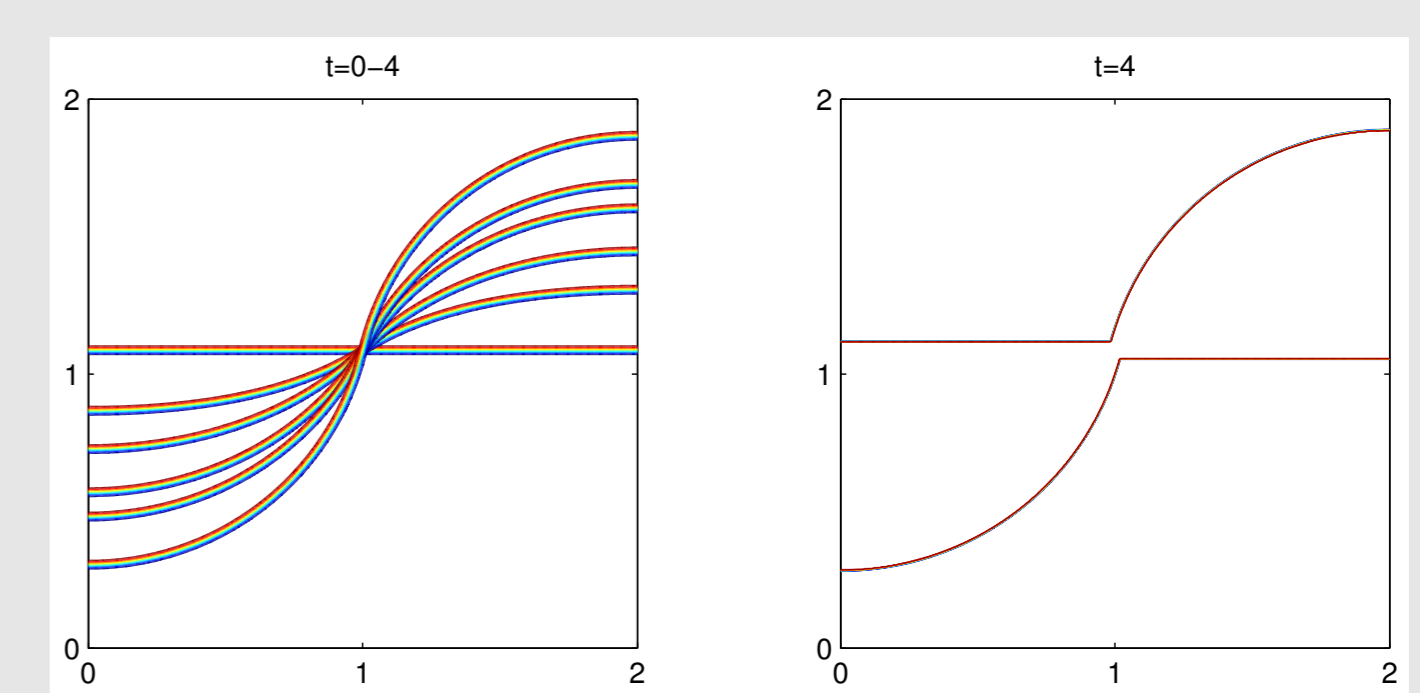


Figure 8: Evolutionary phase field simulation showing a stable S configuration.

◆ Level set model

Let $\omega : \mathbb{R}^2 \times (0, T) \rightarrow \mathbb{R}$ and the zero level set $\Gamma_t = \{\mathbf{x} \in \mathbb{R}^2 : \omega(\mathbf{x}, t) = 0\}$, see [9] then the level set bi-directional model for diffusion induced grain boundary motion takes the form

$$\omega_t - |\nabla\omega| \mathcal{F}[u, \omega] = |\nabla\omega| \nabla \cdot \left(\frac{\nabla\omega}{|\nabla\omega|} \right) \quad (12)$$

$$u(\mathbf{x}, t) = \begin{cases} 1 & \text{if } \exists \bar{t} \leq t : |\omega(\mathbf{x}, \bar{t})| < \varepsilon \\ 0 & \text{otherwise} \end{cases} \quad (13)$$

where $\mathcal{F}[u, \omega] = u(\mathbf{x} + \delta_\omega^+ \mathbf{n}_\omega) - u(\mathbf{x} - \delta_\omega^- \mathbf{n}_\omega)$ and

$$\mathbf{n}_\omega = \frac{\nabla\omega}{|\nabla\omega|}, \quad \delta_\omega^\pm = \min_{r \in \mathbb{R}^+} \{ |\omega(\mathbf{x} \pm r \mathbf{n}_\omega)| = \pm \varepsilon \}.$$

- We solve (12), (13) using a narrow band/re-initialization approach see [9].
- Figure 9 displays the evolution of an initially straight grain boundary spanning Ω that after some time doubles back on itself to form a double seam. The lefthand subplot displays contour plots of the level set solution ω_h at times $t = 0, 2.5, 7.5$ and 4 while the righthand plot displays the concentration u_h at the final time, at time $t = 4$.

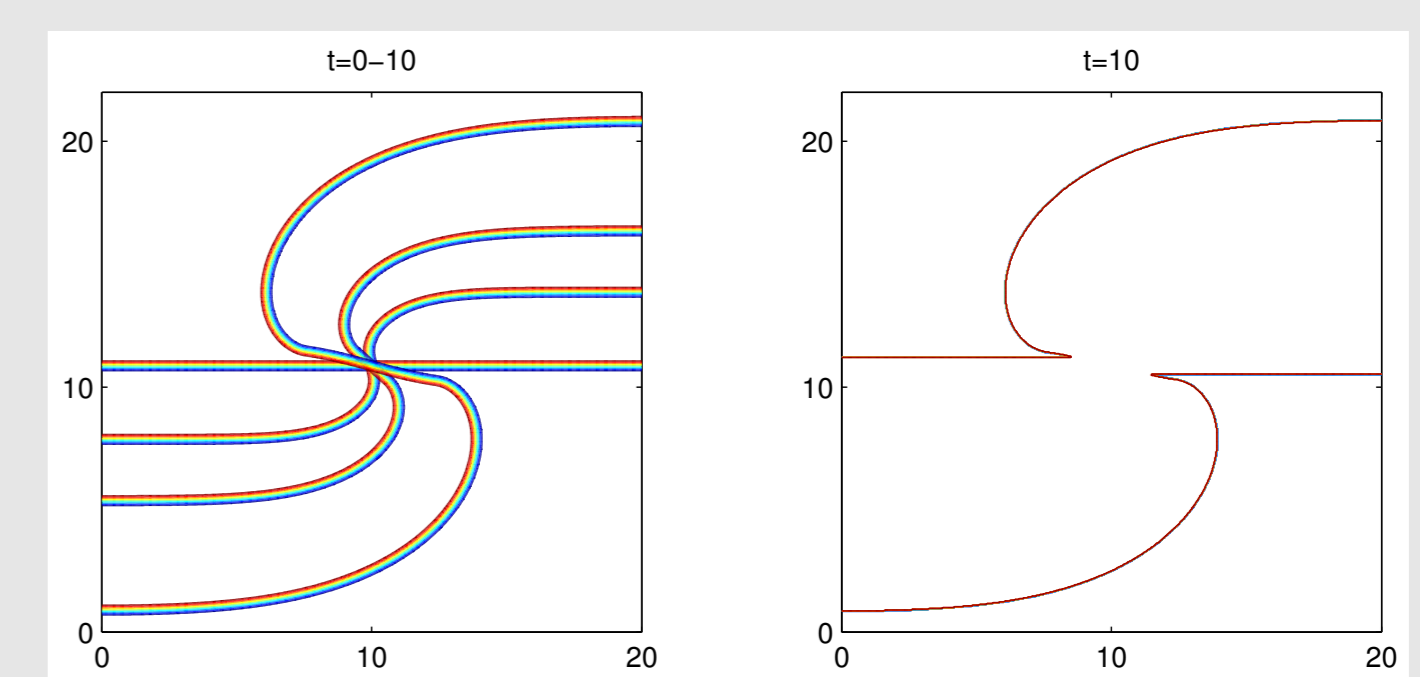


Figure 9: Evolutionary level set simulation showing the formation of a double seam.

References

- [1] CAHN, J.W., FIFE, P. & PENROSE, O. *A phase field model for diffusion-induced grain-boundary motion*. Acta Mater. **45**, (1997) 4397-4413.
- [2] DECKELNICK, K. & ELLIOTT, C.M. *An existence and uniqueness result for a phase field model of diffusion-induced grain-boundary motion*. Proc. Roy. Soc. Edin. Ser. A. **131A** (2001) 1323-1344.
- [3] DECKELNICK, K., ELLIOTT, C.M. & STYLES, V. *Numerical diffusion induced grain boundary motion*. Interfaces and Free Boundaries **3** (2001) 393-414.
- [4] ELLIOTT, C.M. & STYLES, V. *Computations of bi-directional grain boundary dynamics in thin metallic films*. J. Comp. Phys. **187** (2003) 524-543.
- [5] FIFE, P., CAHN, J.W. & ELLIOTT, C.M. *A free boundary model for diffusion-induced grain-boundary motion*. Interfaces and Free Boundaries **3** (2001) 291-336.
- [6] FIFE, P. & WANG, X-P. *Chemically induced grain boundary dynamics, forced motion by curvature, and the appearance of double seams*. Euro. J. Appl. Math. (2002) **13** 25-52.
- [7] HANDWERKER, C. *Diffusion-induced grain boundary migration in thin films*. Diffusion Phenomena in Thin Films and Microelectronic Materials, Ed. D. Gupta and P.S. Ho, Noyes Pubs. Park Ridge, N.J. (1988) 245-322.
- [8] MAYER, U.F. & SIMONETT, G. *Classical solutions for diffusion induced grain boundary boundary motion*. J. Math. Anal. **234**, (1999) 660-674.
- [9] SETHIAN, J.A. *Level set methods and fast marching methods*. Cambridge Monographs on Applied and Computational Mathematics **3**, (1999) Cambridge University Press.